



An experimental study of bouncing Leidenfrost drops: Comparison between Newtonian and viscoelastic liquids

V. Bertola

University of Edinburgh, School of Engineering and Electronics, King's Buildings, Mayfield Road, Edinburgh EH9 3JL, UK

ARTICLE INFO

Article history:

Received 27 August 2008

Available online 4 December 2008

ABSTRACT

The effect of polymer additives on the dynamic Leidenfrost phenomenon (rebound of liquid drops impacting on very hot walls, where a thin vapour cushion separates the liquid from the surface) is studied experimentally by high-speed imaging. Drops of a dilute solution (200 ppm) of Polyethylene Oxide (PEO), with equilibrium diameters of 2.66 and 3.32 mm, were compared with drops of pure water (diameters of 2.76 and 3.49 mm) during the impact on an aluminium surface at a temperature of 400 °C and impact Weber numbers between 7 and 160. The additive causes a slight reduction of the maximum spreading diameter and of the retraction velocity of the drop after impact and, within a certain range of Weber numbers, enhances significantly the maximum height of the drop center of mass during rebound. These results, obtained for a non-wetting case, are different from those previously obtained for impacts on dry surfaces, where polymer additives hardly change the maximum spreading diameter but reduce the retraction velocity of nearly one order of magnitude and completely suppress drop rebound.

© 2008 Elsevier Ltd. All rights reserved.

1. Introduction

When a drop is deposited on a very hot surface, the liquid directly exposed to heat evaporates almost instantaneously, creating a vapour cushion over which the drop floats. Because the thermal conductivity of gases is small compared with that of liquids and solids, the thin vapour film acts as a thermal insulator, which strongly reduces the rate of evaporation of the rest of the liquid: thus, drops deposited on a very hot surface may be observed for several minutes before they evaporate completely. As it is well known, this phenomenon is named after Leidenfrost, who observed it incidentally in 1756 [1], and the minimum temperature of the surface at which it occurs (which is well above the saturation temperature of the liquid) is called the Leidenfrost temperature [2]. To a certain extent, the Leidenfrost phenomenon can be described in terms of a liquid drop on an air cushion [3].

A similar phenomenon can be observed when a drop impacts on the hot surface with a certain velocity: in this case, the vapour film between the drop and the surface not only prevents a rapid evaporation of the liquid, but allows the drop to bounce off the surface [4], which is known as “dynamic Leidenfrost phenomenon” [5]. After the initial spreading that follows impact, the drop retracts to retrieve its spherical shape and minimize its surface energy; however, because of the vapour film the drop does not wet the surface during retraction, which reduces the energy dissipation due to shear flow and leaves more of the initial kinetic energy available for bouncing. Moreover, if the temperature of the surface is very

high, the compressibility of the vapour film and the momentum exchange between the drop and the film are also thought to contribute propelling the drop away from the surface [6].

Roughly speaking, the dynamic Leidenfrost phenomenon occurs for low values of the Weber number (i.e., when the ratio between kinetic energy and surface energy is small enough to prevent the drop from breaking-up into smaller droplets) and temperatures high enough to allow the formation of the vapour film. In general, the wall temperature must be significantly higher than the Leidenfrost temperature for the same fluid/surface combination, because in the dynamic case the vapour film tends to collapse under the combined action of the drop weight and the dynamic pressure rise during impact: thus, a higher rate of evaporation hence a higher wall temperature is required to ensure the stability of the vapour film.

If the vapour film is not stable, for example because the surface temperature is not high enough, the liquid may locally touch the surface and start boiling: then, the small vapour bubbles formed inside the drop quickly rise and burst on the drop surface, scattering all around small satellite droplets, which is known as “secondary atomisation” or “drop miniaturisation” [7]. Thus, one can define a dynamic Leidenfrost temperature as the lowest temperature for which the vapour cushion causes drop bouncing without secondary atomization or splashing. This temperature has been shown to be a growing function of the impact Weber number [8].

From this qualitative overview, one can realise that the dynamic Leidenfrost phenomenon is a rich source of challenging problems for scientists, but at the same time plays a critical role in many practical applications, in particular those concerning spray cooling,

E-mail address: v.bertola@ed.ac.uk

Nomenclature	
a	capillary length
c	heat capacity
D_0	equivalent drop diameter
E_{rec}	energy recovered
g	gravity
H	falling height
H_{max}	maximum height of center of mass
k_{vap}	thermal conductivity of vapour
m	drop mass
RC	restitution coefficient
S	surface exposed to heat
t	time
T	temperature
T_{amb}	ambient temperature
T_{C}	contact time
T_{sat}	saturation temperature
T_{surf}	surface temperature
u	impact velocity
u_{ret}	retraction velocity
We	Weber number
<i>Greek symbols</i>	
δ	vapour layer thickness
η	viscosity
ρ	density
σ	equilibrium surface tension

firefighting, and steel quenching. In most circumstances, drop bouncing has a negative effect on the process, because when the drop is far from the surface the cooling or quenching efficiency greatly reduces.

Although the fluids used in most of these applications are Newtonian, the interest in liquids with non-Newtonian behaviour is rapidly increasing in modern industrial processes. Very often, these fluids are obtained by adding to a Newtonian solvent tiny amounts of flexible polymers, which are sufficient to change the response to external forcing of the fluid (which becomes viscoelastic) without affecting significantly its shear viscosity and surface tension. Polymer additives are known to change substantially the morphology of drop impacts. For example, it has been shown that a small quantity (of the order of 100 ppm) of poly-ethylene oxide (PEO) can reduce the tendency of drops to rebound after impacting on hydrophobic surfaces, which can be exploited to control spray applications [9–11]. In particular, polymer additives completely inhibit secondary atomisation during the impact on hot surfaces, with the result that the “apparent” dynamic Leidenfrost temperature becomes almost identical to that of sessile drops [12].

These effects are believed to be related to the elongational viscosity of the fluid [13], the ratio of the first normal stress difference to the rate of elongation of the fluid, which for a polymer solution can be two or three orders of magnitude higher than that of the solvent [14]. From the microscopic point of view, elongational viscosity is thought to be simply the collective effect of several polymer molecules undergoing a coil-stretch transition [15] due to the hydrodynamic action of the surrounding fluid. At rest, polymer molecules are coiled in a state of maximum conformational entropy, whereas if the hydrodynamic forces are sufficiently large they unfold, opposing an increasing resistance to deformation as they are stretched. In particular, it has been suggested that the elongational viscosity causes large energy dissipations, so that nothing of the impact kinetic energy is available to propel the drop off the surface. This seems to be confirmed by measurements of the retraction velocity of the drop after maximum spreading, which for polymer solutions is about one order of magnitude smaller than that measured for the pure solvent [9,10]. However, although the correlation between the retraction velocity of the lamella and the elongational viscosity seems to be well established, the actual physical mechanism is still far from being understood.

This work aims to investigate the effect of polymer additives on bouncing Leidenfrost drops, for surface temperatures above the dynamic Leidenfrost point (i.e., when no secondary atomisation is observed). Because of the vapour layer between the drop and the surface, wetting effects are negligible: thus, from this study one can also get a deeper insight of the effect of additives on the drop impact dynamics on hydrophobic surfaces.

2. Experiments

2.1. Apparatus and procedure

The experimental setup is schematically shown in Fig. 1. Drops were created at the tip of a hypodermic needle with flattened bevel by a screw-driven syringe dispenser, and detached under their own weight. Two needles with inner diameters of 0.838 mm and 0.495 mm (gauge 18 and gauge 21, respectively) were used to create drops of different diameters. In order to change the impact velocity, the dropping height was adjusted using a Vernier height gauge with a precision of ± 0.02 mm.

The needle was positioned above the surface of an aluminium square block (40 × 40 mm) containing two electric cartridge heaters (100 W each) symmetric with respect to the point of impact to ensure a uniform temperature field. The surface was mirror polished with a chemical abrasive. Temperature could be controlled within ± 1 °C by a PID controller driven by a K-thermocouple placed 1 mm below the point of impact. Drop impacts were recorded for a constant wall temperature of 400 °C, high enough to keep the vapour film stable and avoid the formation of secondary droplets [8,12].

A high-frame rate CMOS camera (Mikrotron MC1310) equipped with a 18–108/2.5 macro zoom lens (Navitar Zoom 7000) and horizontally aligned with the surface recorded the impacts of single drops. Back-to-front illumination was provided by a LED backlight (Advanced Illumination) which ensured a uniform illumination intensity, and images with a resolution of 480 × 480 pixels were captured at 1000 frames per second. Magnification was kept constant throughout all experiments and lengths on the image could be calculated by comparison with a reference length (typical spatial resolution: 35 pixels/mm). To ensure a fine optical alignment, the camera, the heated surface and the backlight were fixed to an optical breadboard.

Quantitative data were extracted from images using proprietary software developed in LabView environment, which after background subtraction and image optimization measured the gap between the drop and the wall, as well as the drop dimensions in the vertical and in the horizontal directions.

2.2. Drop characterization

In this work, drops were created using two different fluids: de-ionized water and a 200 ppm solution of poly-ethylene oxide in the same water. The PEO, supplied by Aldrich Chemicals under the form of granular powder, had an average molecular weight of 4,000,000 amu and a typical density of 1210 kg/m³. The solution

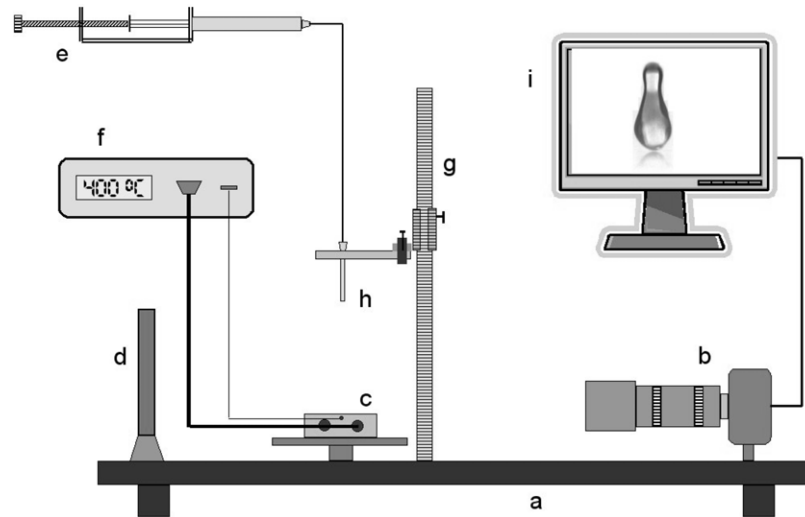


Fig. 1. Schematic of the experimental setup: (a) optical breadboard; (b) high-speed camera; (c) heated aluminium block; (d) LED backlight; (e) drop dispensing system; (f) temperature controller; (g) height gauge; (h) needle; (i) computer.

was prepared by gently dissolving the polymer into a batch of ultra-pure water, where a large vortex was created by a magnetic stirrer, then mixed for about one hour at low speed. This procedure prevents the formation of non-dissolved polymer clusters, which make the solution inhomogeneous, and at the same time minimizes shear degradation.

Drop weight measurements made with a precision balance (Mettler Toledo MT100) allowed calculation of the drop diameter at equilibrium, $D_0 = \sqrt[3]{6m/\pi\rho}$. Statistical measurements over 50 samples gave values of 2.76 ± 0.14 and 3.49 ± 0.04 mm for the diameter of water drops, whereas drops of polymer solution had diameters of 2.66 ± 0.1 and 3.32 ± 0.06 mm, respectively for the gauge 21 and the gauge 18 needles. To characterize the shape of drops, one can compare the drop radius with the capillary length, $a = \sqrt{\sigma/\rho g}$ which is indicative of the competition between surface forces and gravity. If the drop radius is smaller than the capillary length, surface forces will prevail ensuring that the drop has a spherical shape. The capillary length can be used to define a dimensionless diameter, $\bar{D}_0 = D_0/2a$.

To determine the properties of the liquid during the impact (in particular, the surface tension), it is necessary to estimate the drop temperature with a reasonable precision. Because there is a co-existence of the liquid and the vapour phase, if one neglects the pressure wave caused by impact [16] and other non-equilibrium effects, the drop should be at saturation (100 °C for water at atmospheric pressure). However, the impact duration is so short (typically, about 5 ms for the initial spreading phase and about 50 ms for the subsequent retraction phase) that it may not be sufficient to bring whole drop in a condition of uniform temperature, so that only a thin layer of liquid above the vapour film would be at the saturation temperature, while the rest would be colder.

A uniform temperature in the drop can be ensured by using special dispensing systems, for example by containing a Leidenfrost drop for some seconds in the enclosure between an inclined plate and a vertical wall, both of which are kept at the same temperature of the impact surface, before falling by gravity when the vertical wall is removed [17]. However, with such a system controlling the drop diameter would be more difficult.

Since in the present experiments drops are released from the dispensing needle at ambient temperature, it is important to verify whether the duration of the contact with the hot surface is sufficient to heat the drop uniformly at the saturation temperature. A simple energy balance carried out assuming that the main heat transfer mode is thermal conduction in the vapour layer yields:

$$mcdT = \frac{k_{\text{vap}}}{\delta(t)} (T_{\text{surf}} - T)S(t)dt \quad (1)$$

where T is the average temperature of the drop, m its mass, c the heat capacity of water, k_{vap} the thermal conductivity of the vapour layer, $\delta(t)$ its thickness, and $S(t)$ the surface of the drop exposed to the heat flux. To estimate an upper limit for the heating time (worst case), one can make the approximations $S(t) \approx \pi D_0^2/4$ and $\delta(t) \approx \delta_{\text{max}}$, where δ_{max} is proportional to $D_0^{4/3}$ [18], and integrate between the ambient temperature and the saturation temperature:

$$t_h < \frac{2\rho D_0 c \delta_{\text{max}}}{3k_{\text{vap}}} \ln \frac{T_{\text{surf}} - T_{\text{amb}}}{T_{\text{surf}} - T_{\text{sat}}} \quad (2)$$

For a drop with a diameter of 4 mm impinging on a surface at 400 °C, and taking $\delta_{\text{max}} = 50\mu\text{m}$ [18], the time necessary to heat the drop up to the saturation temperature is less than 5 ms, i.e. of the same order of the duration of the expansion phase following impact. Because t_h estimates the heating time in excess, it is reasonable to assume that the drops considered in the present work attain the saturation temperature upon the first contact with the wall, before maximum spreading. Thus, in the following sections the relevant dimensionless numbers will be calculated using the fluid properties at 99 °C.

The surface tension and the viscosity of the polymer solution at saturation were measured by linear extrapolation of values measured in the range 20–80 °C. Viscosities were measured with a rotational rheometer (Haake MARS II) equipped with a 60 mm plate/plate geometry and Peltier temperature controller, while equilibrium surface tensions were measured using a maximum bubble pressure instrument (Krüss PocketDyne). Table 1 summarizes the properties of the fluids and of the drops considered in these experiments. Note that even at 99 °C the capillary lengths of both fluids are still larger than the radii of the drops.

The impact velocity was measured from digital images of falling drops. For small distances of the dispensing needle above the impact surface ($H \leq 15$ cm), it was found to be identical to the theoretical free-fall velocity, $u = \sqrt{2g(H - D_0)}$, as shown in Fig. 2. Thus, the impact Weber number, which expresses the competition between kinetic energy and surface energy, was calculated using the following expression:

$$We = \frac{\rho D_0 u^2}{\sigma} = \frac{2\rho g D_0 (H - D_0)}{\sigma} \quad (3)$$

Table 1
Properties of the drops used in the experiments.

PEO concentration (ppm)	0	0	200	200
Needle gauge	21	18	21	18
Needle inner diameter (mm)	0.495	0.838	0.495	0.838
Needle outer diameter (mm)	0.813	1.270	0.813	1.270
Drop diameter (mm)	2.76 ± 0.14	3.49 ± 0.04	2.66 ± 0.1	3.32 ± 0.06
Density @ 20 °C (kg/m ³)	1000	1000	1000	1000
Density @ 99 °C (kg/m ³)	960	960	960	960
Viscosity @ 20 °C (mPa s)	1	1	1.23	1.23
Viscosity @ 99 °C (mPa s)	0.28	0.28	0.48	0.48
Surface energy @ 20 °C (mJ/m ²)	72	72	70	70
Surface energy @ 99 °C (mJ/m ²)	58	58	54	54
Capillary length (mm)	2.48	2.48	2.39	2.39
Dimensionless diameter	0.56	0.7	0.56	0.7

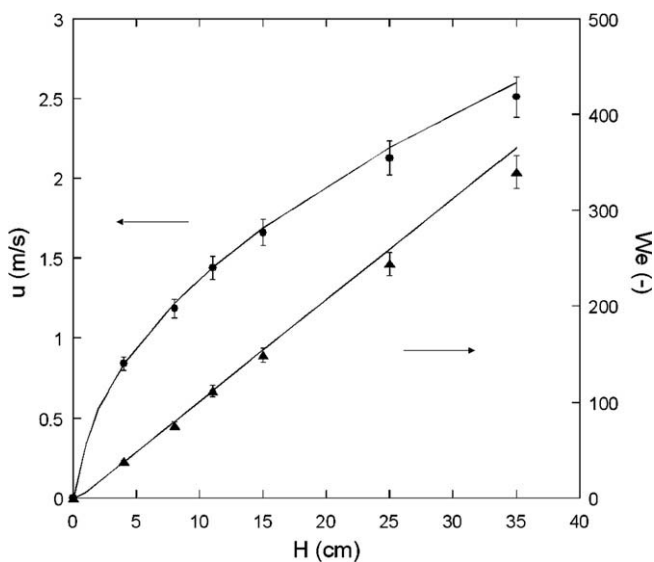


Fig. 2. Comparison between the measured velocity (and the relative Weber number) of impacting drops and the theoretical values obtained for a free-fall (solid lines), for a water drop with $D_0 = 3.49$ mm.

The drops considered in the present work had impact Weber numbers in the range between 7 and 160.

3. Results

3.1. Morphology

When the drop impacts on the surface, it initially spreads forming a disk (sometimes called lamella), which is not in contact with the surface because of the vapour film that forms in the dynamic Leidenfrost regime. Subsequently, the lamella retracts and the drop bounces off the surface, so that it can fall down again and make a new impact, which is replicated until all initial kinetic energy of the drop is dissipated.

Image sequences describing the impacts of different drops are shown in Figs. 3 and 4, respectively for low (<20) and high (>80) Weber numbers. Each sequence shows the drop at five significant instants: (i) the instant of the first impact, (ii) that of maximum spreading, (iii) the moment when the drop takes off from the surface, (iv) when it reaches the maximum height during the first rebound, and (v) when it touches the surface again. Each figure compares two drops of water with two of polymer solution, with different dimensionless diameters.

At low Weber numbers (Fig. 3), the lamella is an almost perfect disk for all drops, irrespective of the size and of the drop viscoelasticity. One can observe, however, that the maximum spreading diameter is slightly smaller for the drops of polymer solution. When drops leave the surface, they exhibit a prolate shape, with mass distributions that can vary significantly from one experiment to another (two meaningful examples are given in images a-3 and d-3 in Fig. 3, where mass is concentrated, respectively, in the lower and in the upper part of the drop). Such large deformations induce waves on the drop surface that persist during flight, so that the drop cannot reach the equilibrium spherical shape. Although this happens for both of the fluids used, the shape of drops of polymer solution looks more symmetric than that of drops of pure water in the same conditions.

At high Weber numbers (Fig. 4), the lamella of water drops exhibits a surface instability on the rim [19,20], which becomes larger as the critical Weber number for splashing is approached. This is less pronounced for viscoelastic drops, where the lamella at maximum spreading looks like a flat disk, similar to drops at lower Weber numbers. The instability of water drops persists and eventually grows during the lamella retraction, contributing to create irregular shapes during flight.

More in general, it appears that the polymer additive smoothes small length-scale deformations of the drop surface during spreading and rebound, while large scale and bulk deformations are unaffected or slightly enhanced. This suggests that the energy distribution and dissipation mechanisms are different for the two fluids.

3.2. Impact and expansion stage

The main physical quantities that characterize the impact stage are the contact time (which here is defined as the time between the first impact and the instant when the drop bounces off the surface, although the drop is always separated from the surface by the vapour film) and the maximum diameter reached by the lamella during the spreading subsequent to impact.

The contact time T_C of non-wetting drops was measured by counting the frames between the drop impact and the instant when the drop leaves the surface, and compared with the value calculated from a balance between inertia and capillarity, which yields $T_C \sim (\rho D_0^3 / \sigma)^{1/2}$ [21]. This means that the contact time scales as $D_0^{3/2}$ and is independent of the impact Weber number, which is confirmed by the results presented in Fig. 5. The polymer additive seems to have no significant effect on this quantity other than that due to the slight reduction of the equilibrium diameter.

Less straightforward is the interpretation of maximum spreading diameter data, which are plotted in Fig. 6 with respect to the impact Weber number. Theories based on the conservation of energy [19,22] suggest that this quantity should scale as $We^{1/2}$. However, more recently it has been proposed that for $We \gg 1$ a model based on the conservation of momentum is more accurate, because it is difficult to quantify energy dissipation during impact [17,23]. Whilst the latter approach seems to be supported by the trends obtained for water drops, in particular for $We > 30$, the maximum spreading diameter of drops containing the polymer additive strictly follows the trend predicted by the conservation of energy approach.

In any case it must be observed that for $We > 20$ the maximum spreading diameter of viscoelastic drops is systematically smaller than that of water drops having the same impact Weber number. This means that the fraction of impact kinetic energy (which is proportional to the Weber number) converted into surface energy (which is proportional to the area of the drop surface at maximum spreading) is smaller.

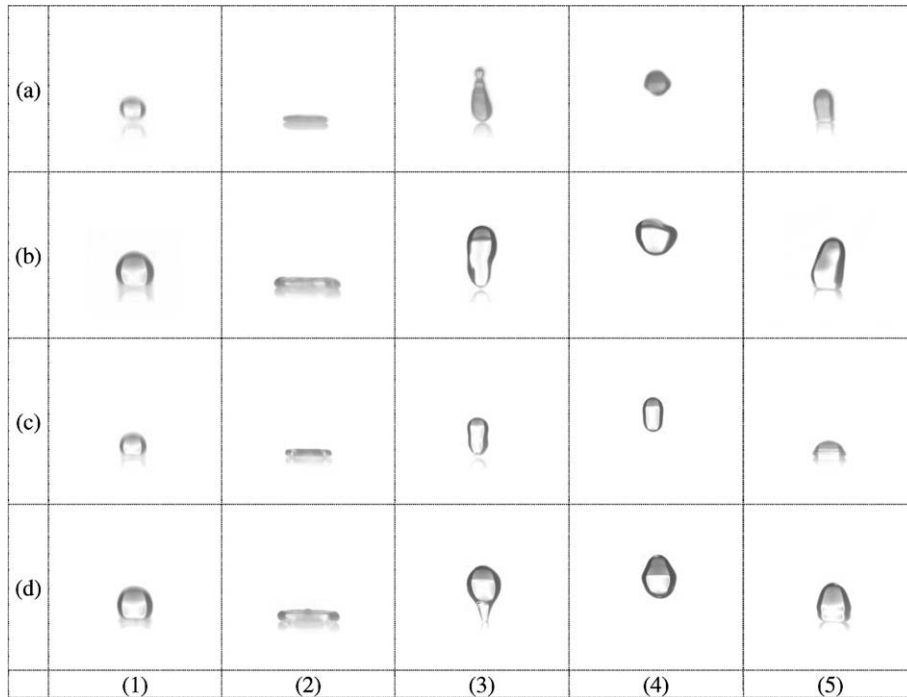


Fig. 3. Morphology of impact and first rebound at low Weber numbers in five significant moments: (1) initial impact, (2) maximum spreading, (3) take-off, (4) maximum height, (5) landing. (a) Water, $\bar{D}_0 = 0.56$, $We = 15.5$; (b) water, $\bar{D}_0 = 0.7$, $We = 18.7$; (c) polymer solution, $\bar{D}_0 = 0.56$, $We = 16.1$; (d) polymer solution, $\bar{D}_0 = 0.7$, $We = 19.3$.

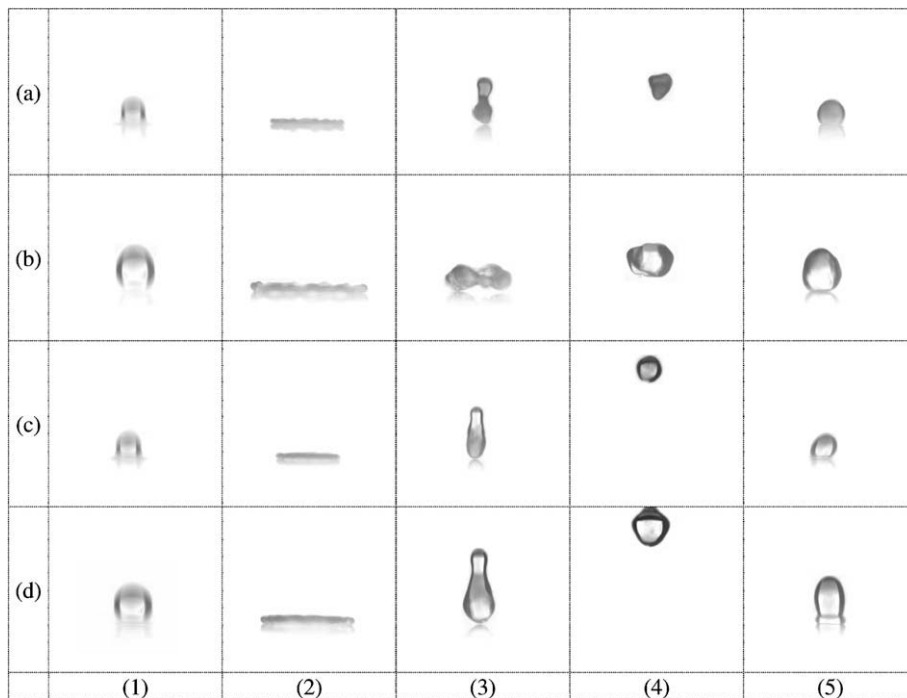


Fig. 4. Morphology of impact and first rebound at high Weber numbers in five significant moments: (1) initial impact, (2) maximum spreading, (3) take-off, (4) maximum height, (5) landing. (a) Water, $\bar{D}_0 = 0.56$, $We = 87.2$; (b) water, $\bar{D}_0 = 0.7$, $We = 86.7$; (c) polymer solution, $\bar{D}_0 = 0.56$, $We = 90.3$; (d) polymer solution, $\bar{D}_0 = 0.7$, $We = 88.8$.

In principle, such reduction of the surface energy at maximum spreading could be interpreted as the consequence of increased dissipation during the expansion stage due to the higher elongational viscosity of the polymer solution, providing an independent confirmation of the theory proposed to explain why polymer additives cause the suppression of drop rebound on hydrophobic surfaces [8], [9] and [12]. However, this does not exclude that the missing surface energy may be stored elsewhere, for example as elastic energy. It must be also remarked that the maximum spread-

ing diameter reduction is quite small, which implies that the effect of the polymer on the bulk elongational properties of the fluid is not as large as it could be expected.

3.3. Retraction and rebound stage

In Newtonian drops, after maximum spreading surface energy is converted back to kinetic energy and propels the drop off the surface. This stage is characterized by the retraction velocity of the la-

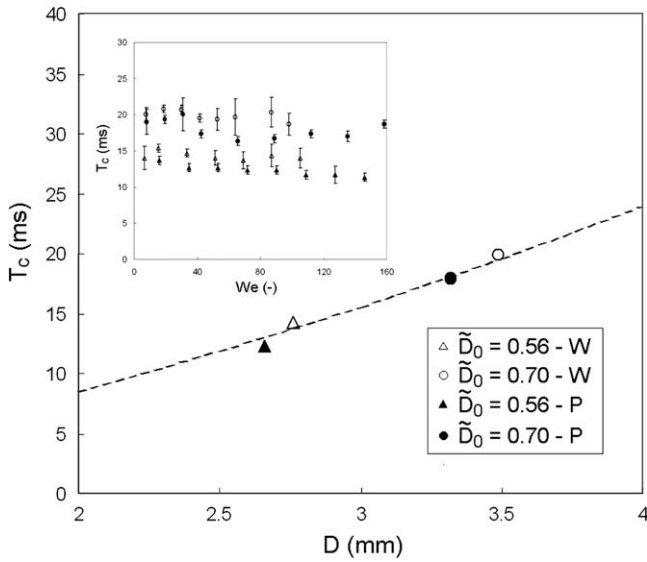


Fig. 5. Contact time of bouncing Leidenfrost drops as a function of the equilibrium diameter, and of the impact Weber number (inset). The discontinuous line represents the scaling law $T_c \sim D_0^{3/2}$, with a pre-factor equal to 3.

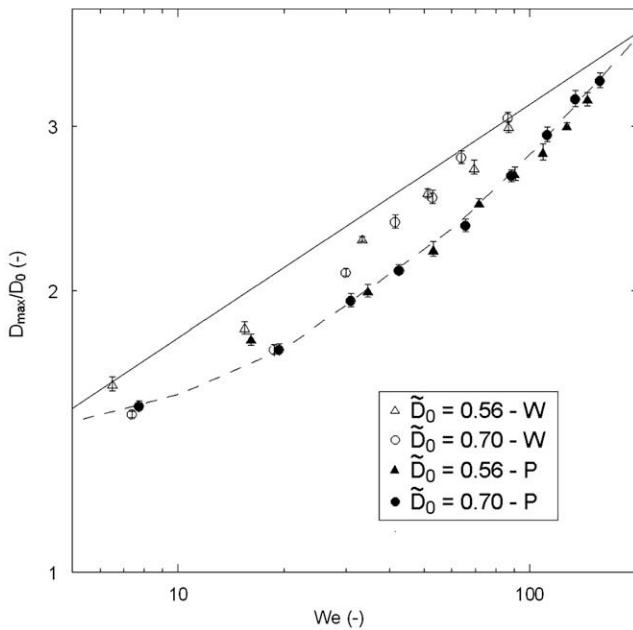


Fig. 6. Maximum spreading diameter of Leidenfrost drops of pure water (open symbols) and polymer solution (filled symbols), impacting on an aluminium surface ($T = 400^\circ\text{C}$). The solid and dashed lines represent the trends $D_{max}/D_0 \sim We^{1/4}$ and $D_{max}/D_0 \sim We^{1/2}$, respectively.

mella, which can be measured by plotting the drop diameter with respect to time and calculating the slope of the curve after the maximum [10]. This quantity plays a major role in the phenomenon of drop rebound, because drops will bounce only if the lamella retraction is fast enough, and no rebound can be observed if the retraction velocity is lower than a certain value. Polymer additives are known to retard the retraction of drops impacting either on hydrophobic, homothermal surfaces [10] or on metallic surfaces heated below the Leidenfrost point [11], causing a retraction velocity decrease of nearly one order of magnitude. While these results were obtained for drops impacting of dry surfaces of different wettability, in the present experiments the effects of wetting are excluded due to the vapour film between the drop and the surface. Thus, it is possible to isolate those effects that are due to a change

in the bulk elongational properties of the fluid caused by the polymer, i.e. a change in the elongational viscosity.

Fig. 7 shows that although the polymer additive causes indeed a reduction of the retraction velocity with respect to pure water, the values measured for the two fluids have the same order of magnitude, with a maximum difference of 27% measured for $We \approx 40$. This is much less than the reduction observed in experiments where drops wet the impact surface [9–11,13]. Similar results were obtained by studying drop impacts on small targets (which is another way to remove the influence of the substrate): there was no retardation of the retraction, and the polymeric lamellae retracted in the same manner as the water lamella [24]. These findings prove that polymeric additives have only limited effects on the elongational deformations of the drop, whereas they may affect significantly its dynamic wetting behaviour. Moreover, the fact that viscoelastic drops have a smaller retraction velocity suggests that the fraction of the impact kinetic energy which might be stored as elastic energy is not converted back to mechanical energy at this stage.

It is interesting to observe that as long as the impact Weber number is not too high and the lamella shape can be approximated by a disk, the retraction velocity is approximately a linear function of the Weber number, with a slope coefficient which is almost the same for the two fluids (the linear best fit gives 6.6 for water drops and 6.9 for the polymer solution, respectively, for retraction velocity in mm/s).

As the critical Weber number for splashing is approached, large instabilities grow around the outermost perimeter of the lamella [20], so that the disk shape is no more a good approximation. In these cases, the value of the retraction velocity drops abruptly.

After the retraction of the lamella is completed, the drop bounces off the surface. The most important quantity characterizing this stage is the maximum height reached by the centre of mass of the drop, because it allows one to calculate exactly the fraction of energy recovered as mechanical energy:

$$E_{rec} = mgH_{max} \quad (4)$$

Fig. 8 shows the maximum height of the drop centre of mass during rebound. For $We \leq 50$, no significant differences can be observed between drops of pure water and viscoelastic drops. On the

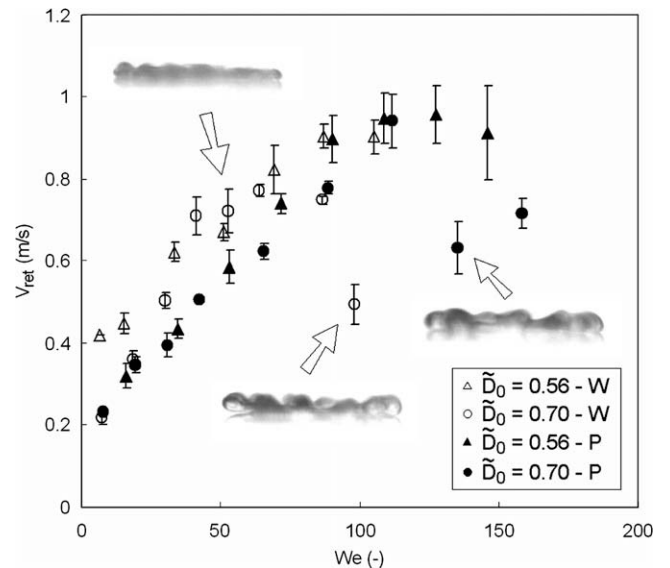


Fig. 7. Retraction velocity after maximum spreading of Leidenfrost drops of pure water (open symbols) and polymer solution (filled symbols), impacting on an aluminium surface ($T = 400^\circ\text{C}$). Inset figures show that at Weber numbers close to the splashing threshold large surface deformations cause a sudden velocity reduction.

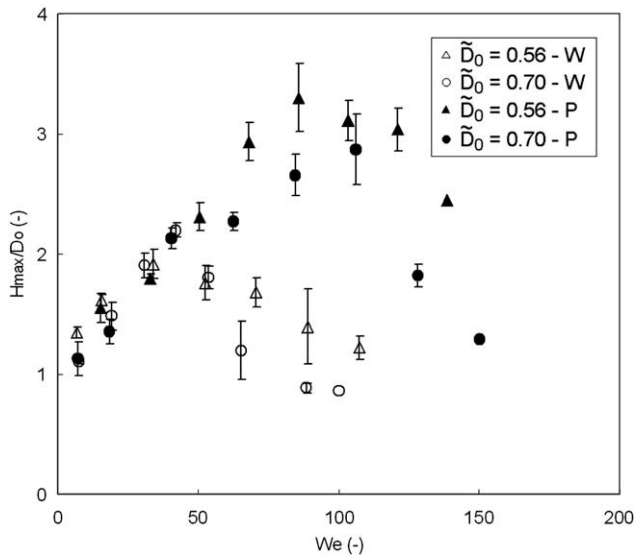


Fig. 8. Maximum height reached by the centre of mass Leidenfrost drops of pure water (open symbols) and polymer solution (filled symbols), after bouncing on an aluminium surface ($T = 400\text{ }^{\circ}\text{C}$).

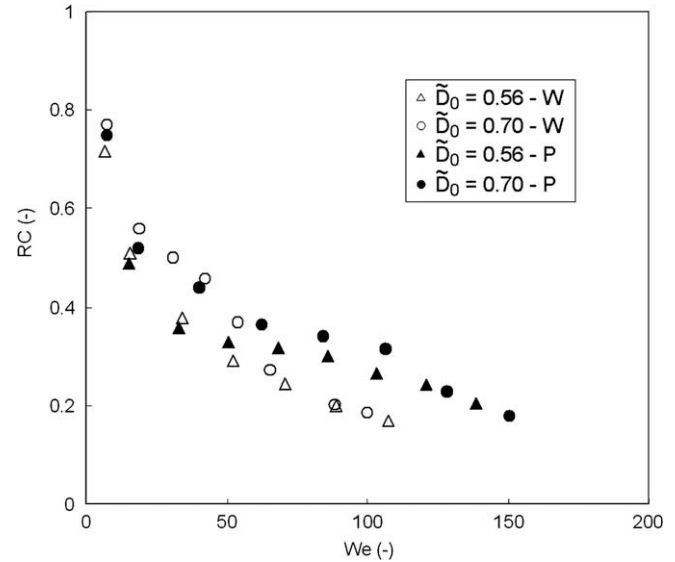


Fig. 9. Restitution coefficient ($RC = v_{\text{rebound}}/u$) of Leidenfrost drops of pure water (open symbols) and polymer solution (filled symbols), impacting on an aluminium surface ($T = 400\text{ }^{\circ}\text{C}$). Error bars are omitted for clarity.

contrary, for $We > 50$ the maximum height reached by viscoelastic drops is significantly larger than that of Newtonian drops, irrespective of the drop diameter.

These results are somewhat surprising, because they clearly show that viscoelastic drops can recover a higher fraction of the initial impact kinetic energy even if they store less in the form of surface energy, and even if the retraction velocity of the lamella is smaller (which also rules out the role of elastic energy stored during the lamella expansion). This seems to be in contrast with the scenario of higher energy dissipation in the fast elongational flow of polymer solutions described above [8,9,12].

The energy recovery of the drop after impact is often characterized by the so-called restitution coefficient, which is defined as the ratio between the rebound velocity and the impact velocity of the drop. Thus, the restitution coefficient corresponds to the square root of the fraction of energy recovered after impact. Because during rebound there are no forces acting on the drop except gravity, the rebound velocity can be estimated from the duration of the rebound itself, i.e. from the time during which the drop is not in contact with the wall [17]. However, in the present work this method would prove difficult, because as one can see from Figs. 3 and 4 drops undergo large deformations, so that the center of mass is not at the same height at the beginning and at the end of rebound. Thus, the rebound velocity has been estimated from the maximum height of the center of mass as:

$$v_{\text{rebound}} = \sqrt{2gH_{\text{max}}} \quad (5)$$

Fig. 9 confirms that for $We > 50$ the restitution coefficient of viscoelastic drops is higher than that of Newtonian drops, while no significant differences can be observed for $We < 50$. This obviously implies that the overall energy dissipation during the impact of viscoelastic drops is smaller.

Since these results have been obtained in a perfectly non-wetting case, one can argue that the suppression of rebound observed in drops of dilute polymer solutions impacting on hydrophobic surfaces is not due to the higher energy dissipation during impact, but rather to some still poorly understood effect of flexible polymers on the dynamic wetting behaviour of drops.

4. Conclusions

Small amounts of flexible polymers dissolved into a Newtonian solvent were shown to have significant effects on the behaviour of bouncing Leidenfrost drops. In particular, additives were shown to affect:

- the impact morphology, smoothing small deformations of the drop surface during spreading and rebound;
- the maximum spreading diameter, which is systematically smaller than for drops of the pure solvent;
- the retraction of the lamella, which is slightly slower for the polymer solution;
- the maximum height of rebound, which is significantly enhanced at Weber numbers greater than 50.

Although a complete understanding of these effects remains elusive at present, it seems that polymers reinforce the stability of the drop free surface, and change the mechanisms of energy distribution and dissipation in the fluid. The enhancement of drop rebound observed for polymer solutions in a certain range of Weber numbers suggests that the overall mechanical energy dissipation during impact is smaller than that of Newtonian drops.

These results are in apparent contradiction with some well-known effects of polymer additives, which have been shown to reduce the retraction velocity of drops impacting on hydrophobic surfaces of nearly one order of magnitude, and to completely suppress the drop rebound. So far, such effects have been understood as a consequence of the higher energy dissipation in the viscoelastic fluid due to its increased elongational viscosity.

However, the experiments described in the present work are not affected by wetting, due to the presence of the vapour film between the liquid and the surface. Thus, the results show the actual effect of the change of the bulk elongational properties of the fluid. This allows one to conclude that the change of the elongational viscosity of the fluid plays only a marginal role in causing the suppression of drop rebound on hydrophobic surfaces, while the different dynamic wetting behaviour of polymer solutions is probably the major cause of this phenomenon.

Acknowledgments

The author thanks D. Quéré for many useful discussions. Financial support from the EPSRC (EP/E005950/1) is gratefully acknowledged.

References

- [1] J.G. Leidenfrost, On the fixation of water in diverse fire, *Int. J. Heat Mass Transfer* 9 (1966) 1153–1166.
- [2] J.D. Bernardin, I. Mudawar, The Leidenfrost point experimental study and assessment of existing models, *J. Heat Transfer (Trans. ASME)* 121 (1999) 894–903.
- [3] M.A. Goldshtik, V.M. Khanin, V.G. Ligai, A liquid drop on an air cushion as an analogue of Leidenfrost boiling, *J. Fluid Mech.* 166 (1986) 1–20.
- [4] L.H.J. Watchers, N.A.Y. Westerling, The heat transfer from a hot wall to impinging water drops in the spheroidal state, *Chem. Eng. Sci.* 21 (1966) 1047–1056.
- [5] B.S. Gottfried, C.J. Lee, K.J. Bell, The Leidenfrost phenomenon: film boiling of liquid droplets on a flat plate, *Int. J. Heat Mass Transfer* 9 (1966) 1167–1188.
- [6] M. Rein, Interactions between drops and hot surfaces, in: M. Rein (Ed.), *Drop-Surface Interactions*, CISM Courses and Lectures, vol. 456, Springer, Berlin, Heidelberg, New York, 2003, pp. 5–89.
- [7] J.D. Naber, P.V. Farrell, Hydrodynamics of droplet impingement on a heated surface, *SAE 930919* 5 (1993) 1–16.
- [8] S.-C. Yao, K.Y. Cai, The dynamics and Leidenfrost temperature of drops impinging on a hot surface at small angles, *Exp. Thermal Fluid Sci.* 1 (1988) 363–371.
- [9] R. Crooks, D.V. Boger, Influence of fluid elasticity on drops impacting on dry surfaces, *J. Rheol.* 44 (2000) 973–996.
- [10] V. Bergeron, Designing Intelligent Fluids for Controlling Spray Applications, *C.R. Physique* 4 (2003) 211–219.
- [11] V. Bertola, Drop impact on a hot surface. Effect of a polymer additive, *Exp. Fluids* 37 (2004) 653–664.
- [12] V. Bertola, K. Sefiane, Controlling secondary atomization during drop impact on hot surfaces by polymer additives, *Phys. Fluids* 17 (10) (2005) 108104.
- [13] R. Crooks, J. Cooper-White, D.V. Boger, The role of dynamic surface tension and elasticity on the dynamics of drop impact, *Chem. Eng. Sci.* 56 (2001) 5575–5592.
- [14] R.F. Bird, C.F. Curtiss, R.C. Armstrong, O. Hassager, *Dynamics of Polymeric Liquids*, Wiley, New York, 1987.
- [15] P.-G. De Gennes, Coil-stretch transition of dilute flexible polymers under ultrahigh velocity gradients, *J. Chem. Phys.* 60 (12) (1974) 5030–5042.
- [16] M. Lesser, The impact of a compressible liquid, in: M. Rein (Ed.), *Drop-Surface Interactions*, CISM Courses and Lectures, vol. 456, Springer, Berlin, Heidelberg New York, 2003.
- [17] A.-L. Biance, F. Chevy, C. Clanet, G. Lagubeau, D. Quéré, On the elasticity of an inertial liquid shock, *J. Fluid Mech.* 554 (2006) 47–66.
- [18] A.-L. Biance, C. Clanet, D. Quéré, Leidenfrost drops, *Phys. Fluids* 15 (6) (2003) 1632–1637.
- [19] M. Rein, Phenomena of liquid drop impact on solid and liquid surfaces, *Fluid Dynam. Res.* 12 (1993) 61–93.
- [20] A.L. Yarin, Drop impact dynamics: splashing, Spreading, receding, bouncing, *Annu. Rev. Fluid Mech.* 38 (2006) 159.
- [21] D. Richard, C. Clanet, D. Quéré, Contact time of a bouncing drop, *Nature* 417 (2002) 811.
- [22] S. Chandra, C.T. Avedisian, On the collision of a droplet with a solid surface, *Proc. R. Soc. Lond. A Math. Phys. Eng. Sci.* 432 (1991) 13–41.
- [23] C. Clanet, C. Béguin, D. Richard, D. Quéré, Maximal deformation of an impacting drop, *J. Fluid Mech.* 517 (2004) 199–208.
- [24] A. Rozhkov, B. Prunet-Foch, M. Vignes-Adler, Impact of drops of polymer solutions on small targets, *Phys. Fluids* 15 (2003) 2006–2019.